Quantitative multiphoton imaging for guiding basal-cell carcinoma removal

Sung-Jan Lin[1], Chih-Jung Hsu[1], Ruei-Jr Wu[2], Chien-Jui Kuo[2], Jau-Shiuh Chen[1], Jung-Yi Chan[1,3], Wei-Chou Lin[4], Shiou-Hwa Jee[1], Chen-Yuan Dong[2]

1. Department of Dermatology, National Taiwan University Hospital and College of Medicine, Taipei, Taiwan.
2. Department of Physics, National Taiwan University, Taipei, Taiwan.
3. Department of Dermatology, Cathay General Hospital, Taipei, Taiwan
4. Department of Pathology, National Taiwan University, Taipei, Taiwan

Abstract

For secure removal of the basal cell carcinoma tissue, the technique of Mohs' micrographic surgery is often used. However, Mohs' micrographic surgery is time-consuming. In this work, we evaluate the ability of multiphoton fluorescence (MF) and second harmonic generation (SHG) imaging to discriminate the borders of human basal cell carcinoma. Morphologically, basal cell carcinomas are featured by clumps of autofluorecent cells with relatively large nuclei and marked peripheral palisading in the dermis. In contrast, SHG from collagen contributes largely to the multiphoton signal in normal dermis. Within the cancer stroma, SHG signals diminish and are replaced by autofluorescent signals. The results suggest that normal collagen structures responsible for SHG have been altered in the cancer stroma and may reflect an up-regulated collagenolytic activity of cancer cells. To better delineate the cancer cells and cancer stroma from normal dermis, a quantitative MF to SHG index (MFSI) is developed. We demonstrate that this index can be used to differentiate cancer cells and adjacent cancer stroma from normal dermis. Our work shows that MF and SHG imaging can be an alternative for the real-time guidance of the secure removal of basal cell carcinoma.

Keywords: basal cell carcinoma, multiphoton, fluorescence, second harmonic generation, collagen, Mohs' micrographic surgery

Photonic Therapeutics and Diagnostics III, edited by Nikiforos Kollias, Bernard Choi, Haishan Zeng, Reza S. Malek, Brian J. Wong, Justus F. R. Ilgner, Kenton W. Gregory, Guillermo J. Tearney, Henry Hirschberg, Steen J. Madsen, Proc. of SPIE Vol. 6424, 642404, (2007) · 1605-7422/07/$18 · doi: 10.1117/12.699891

Address correspondence to: S.H.J. at shiouhwa@ha.mc.ntu.edu.tw and
C.Y.D. at cydong@phys.ntu.edu.tw

1. Introduction

Basal cell carcinoma (BCC) is the most common type of skin cancers.[1] It is estimated that there are about 800,000 new cases of BCC per year in the US,[1] with an annual incidence rate of nearly 200 for every 100,000 women and 400 for every 100,000 men.[1] Photodamage caused by excessive sunlight exposure is an important risk factor for this cancer. BCC most often develops on the head and neck regions of patients where accumulative sunlight exposure is highest as compared with other body surface. Though rarely metastasizing, basal cell carcinoma can be locally destructive. Usually, surgical removal is recommended for patients with BCC. Usually simple excision is employed for removal of BCC. However, even excised with a safety margin clinically, the microscopic margin of cancer can not be securely determined and local recurrence rate can be higher than 10% in cases undergoing simple excision.

Further, when BCC develops in certain anatomical sites including the nose and eyelids, simple excision with a wide margin may not be suitable for the purpose of preserving these important structures.

To remove the entire BCC tissue securely, the technique of Mohs' micrographic surgery was developed. This technique can detect cancer margin with approximately 100% certainty and the recurrence rates are only 1%.[2] However, Mohs' micrographic surgery is time-consuming. In addition, it requires the simultaneous cooperation of the technician for specimen processing and the surgeon. The excised specimen is marked and immediately processed for histological examination. If residual cancerous tissue is observed on the margin of the specimen, further excision of the tumor is performed and the excised specimen is immediately processed again for histological examination. The procedures are repeated until no cancerous tissue is revealed microscopically. This limits the wide application of Mohs' micrographic surgery and Mohs' micrographic surgery is only available in special institutions. Therefore, the development of a minimally-invasive technique capable of real-time determination of BCC margins to circumvent the above mentioned drawbacks is invaluable to clinical dermatology.

Multiphoton fluorescence (MF) microscopy employing ultrafast laser for non-linear excitation of fluorescent materials has been widely used for biological

specimen imaging both in vivo an in vitro.[3-7] Due the non-linear excitation process, only the focal volume can be effectively excited by use of near-infrared light source, allowing higher axial contrast, increased imaging depth and lower overall sample photodamage. In addition, the easy access to the emitted fluorescence also enables further analysis of the features of emitted light, such as fluorescence spectrum and fluorescence life time, to be determined.[3,8] Further, another non-linear optical effect of second harmonic generation (SHG) has also been widely used in biomedical imaging also.[8-10] Briefly, the interaction of incident laser with biological structures with non-centrosymmetrism, such as collagen, muscle fibers and microtubules, leads to the generation of photons at a wavelength of exactly half the wavelength of the incident light.[8-10] In the process of SHG, no molecular transition is involved and the sample photo-damage is minimal. Since SHG is structurally sensitive, transitions of biomolecular structures can be monitored.[8-13] The abundant collagen fibers in the dermis are capable of generating second harmonic generation (SHG) signals and can provide contrast to other important structures in the dermis. These two techniques, minimally destructive and not relying on the use of exogenous labeling and sample pretreatment, are highly suitable for in vivo application. In this study, we attempted to characterize the non-linear optical properties of BCC and to evaluate the ability of the combination of MF and SHG imaging to discriminate the human BCC from normal dermis.

2. Materials and methods

The MF and SHG microscopic system used in this study is a modified version of a home-built laser scanning microscopic imaging system based on an upright microscope (E800, Nikon, Japan) described previously.[4] A DPSS laser (Millennia X, Spectra Physics, Mountain View, CA) pumped titanium-sapphire laser system (Tsunami, Spectra Physics) was used as the excitation source. The 760 nm output of the laser system was used. Prior to entering the microscope, the excitation source was angularly deflected by a x-y scanning system (Model 6220, Cambridge Technology, Cambridge, MA). The input of the upright microscope was modified to accommodate a beam expander. The excitation source was beam expanded and reflected toward the focusing objective (Nikon S Fluor 40x, NA 1.30). The average laser power at the sample is 4.5 mW. The non-linear MF and SHG signal were generated at the sample focal plane and collected in the epi-illuminated geometry by the same focusing

objective. After passing through the dichroic mirror, the MF and SHG signals were separated into two separate channels where they are detected by independent photomultiplier tubes (R7400P, Hamamatsu, Japan). The SHG signal was isolated by an additional filter centered at 380 nm with a bandwidth of 20 nm while the MF was detected by a band pass filter (435-700nm). The signal photons were processed by a single-photon counting PMT (R7400P, Hamamatsu, Japan) and a home-built discriminator.

The study protocol was approved by our Institutional Review Board. We conformed to the Helsinki Declaration with respect to human subjects in biomedical research. Nodular type formalin-fixed BCC samples are imaged in this study. For comparison MF/SHG images of the cells and tissue with histological results, serial thin cross-section slices (7-10 μm in thickness) of each specimen were used for multiphoton imaging and histological examinations. A thin cross-section slice of each specimen was mounted on the slide and covered with a No. 1.5 coverslip for viewing. Large area multiphoton imaging was performed for each specimen.

3. Results

Figure 1 shows the MF/SHG image of normal skin. In the epidermis, the cytoplasm of keratinocytes is effective in generating MF signals and the nuclei are characterized by a halo in the fluorescent cytoplasm. The epidermis is deficient of SHG signals. In the dermis, SHG contributes to most of the signal. The presence of SHG indicates the regular packing of collagen molecules in the dermis. This reflects the fact that collagen is the major extracellular matrix protein in the dermis. SHG signals can be used to analyze the dermal fibrous structures of collagen. In addition, there are also fine fluorescent elastic fibers penetrating in the SHG-generating collagen fibers (arrow, **Figure 1**).

Figure 2 shows the MF/SHG image of a representative BCC specimen. Within the tumor regions, clumps of fluorescent cancer cells can be visualized. In the magnified image (**Figure 3**), cells with relatively large nuclei can be found and the peripheral cells in each cancer clump are palisading along the basement membrane, a unique feature of basal cell carcinoma. This is consistent with the histological results (**Figure 4**). In the cancer stroma, the SHG signals are greatly diminished and MF signals increase in comparison with that of normal stroma. Since the SHG signals of

collagen depends on the regular packing of triple-helical collagen molecules, the diminished SHG signals in the cancer stroma indicate that the collagen structures responsible for SHG are disrupted or collagen molecules themselves are deficient. Our result is consistent with previous report that collagen content in the BCC stroma is decreased as compared with normal dermal stroma.[14] It has also been shown that matrix metalloproteinase expression is up-regulated in basal cell carcinoma,[15] and the collagenolytic activity may lead to the disruption of collagen in the adjacent stroma. Elastic fiber stains reveal no increased elastic fibers in the cancer stroma (data not shown).

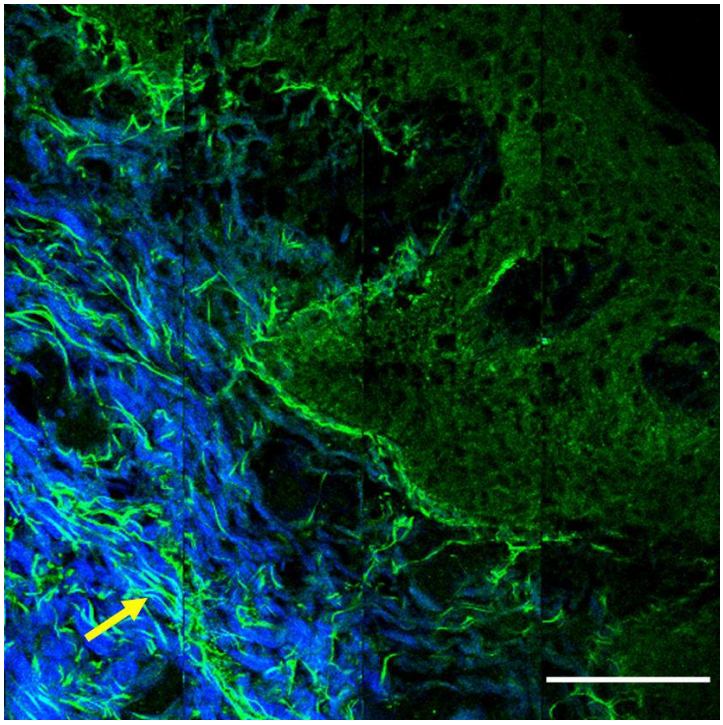

Figure 1. Selected large area multiphoton fluorescence and SHG images of normal skin. In the epidermis, keratinocytes are autofluorescent. SHG signals contribute to most of the dermal signals and some fine autofluorescent fibers are penetrating in the SHG generating dermal stroma (arrow). (bar: 100μm)

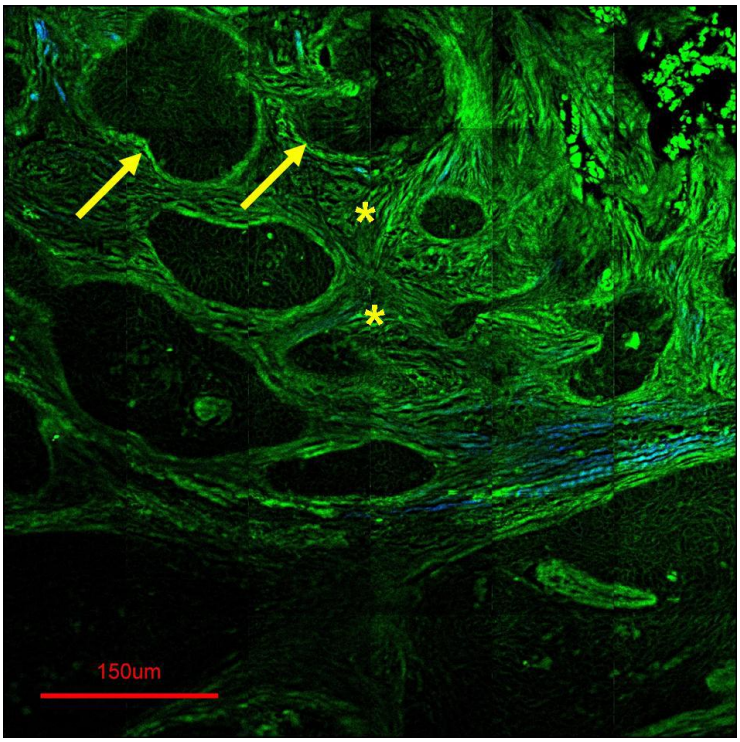

Figure 2. Selected large area multiphoton fluorescence and SHG images of basal cell carcinoma. There are clumps of cancer cells (arrows) embedded in a stroma with decreased SHG signals (stars). (bar: 150μm)

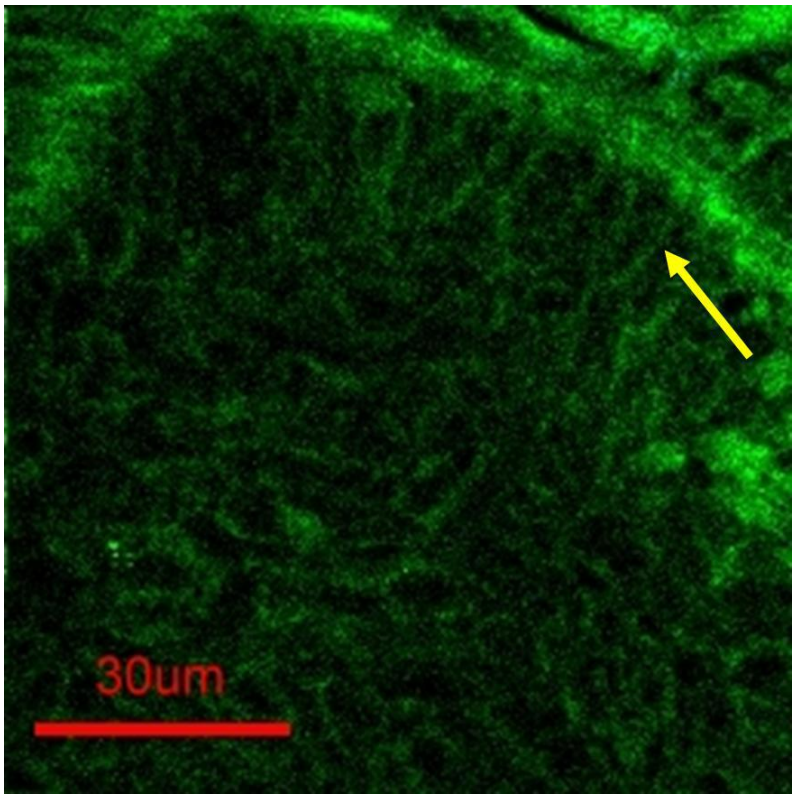

Figure 3. Enlarged image of the basal cell carcinoma clump. Cells have enlarged nuclei and are palisading at the periphery. (bar: 30μm)

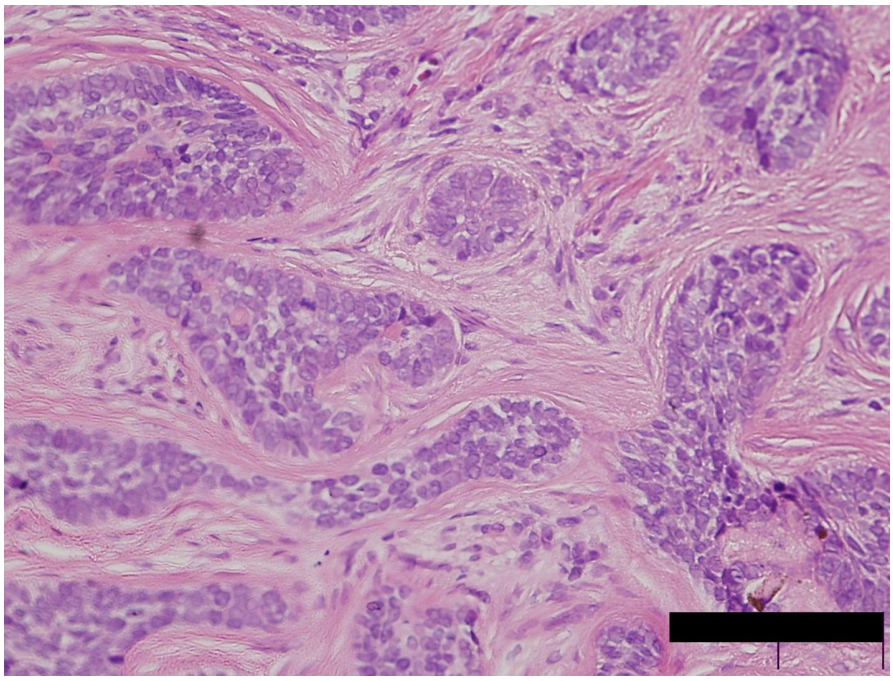

Figure 4. Histology of basal cell carcinoma. Basal cells are characterized by clumps of basaloid cells in the dermis. (bar: 100μm)

However, to help to discriminate BCC from normal dermal stroma, we propose to use the definition of MF to SHG index (**MFSI**). The **MFSI** is defined as:

$$\mathbf{MFSI= (a-b)/(a+b)}$$

In each selected area, the pixels of MF are defined as **a** and pixels of SHG are defined as **b**. In this nomenclature, a highly fluorescent sample (relative to SHG signal) would have a higher MFSI while a specimen containing intense SHG signal (compared with MF) would have a lower MFSI. MFSI approaches the maximum value of 1 when only MF signals are present. The smallest value of MFSI is -1 and this occurs when MF is absent and only SHG signal is present. The index of each selected area is computed and the average index in each case is calculated.

For quantitative analysis of the specimens by use of MFSI, we randomly selected five 50μm by 50μm rectangular areas inside the cancer masses, cancer stroma and normal stroma in the dermis respectively in each sample for quantitative analysis. Cancer stroma includes stroma within the cancer clumps and right adjacent to the cancer mass. Normal stroma is defined as the dermal stroma at least 200μm away from the margin of the tumor clumps.

The MFSI is highest within the tumor masses (mean MFSI=0.93) where the

contribution of the fluorescent signal comes from the cytoplasm. In the normal dermal stroma, the MFSI is the lowest (mean MFSI=0.37), indicating the relative high content of intact collagen molecules. In the cancer stroma, the MFSI (mean MFSI=0.81) is significantly higher than that of normal dermal stroma. The decrease of SHG and increase of MF in cancer stroma accounts for the higher MFSI in comparison with that of normal dermal stroma. Hence, MFSI mapping can help to discriminate normal dermis from BCC cancer and BCC stroma.

4. Discussion

This study shows that multiphoton imaging is able to discriminate BCC from normal dermis. BCCs are featured by clumps of autofluorescent cells with relatively large nuclei and marked peripheral palisading in multiphoton imaging. Compared with normal dermis, the SHG signals decrease and MF signals increase in the stroma within and adjacent to the tumor masses. This reflects higher collagenolytic activity of BCC. We also develop a quantitative analytical index of MFSI which can help to differentiate normal dermal stroma from BCC cells and BCC stroma. Our work shows that, with further development, the combination of MF and SHG imaging can be an alternative for Mohs' surgery in real-time monitoring BCC removal.

Acknowledgement

Support for this work is provided by the National Research Program for Genomic Medicine of the National Science Council, Taiwan. Address correspondence to Dr. Shiou-Hwa Jee at shiouhwa@ha.mc.ntu.edu.tw and Dr. Chen-Yuan Dong at cydong@phys.ntu.edu.tw.

References

1. Rubin AI, Chen EH, Ratner D. Basal cell carcinoma. N Engl J Med 353:2262-9, 2005.
2. Rowe DE, Carroll RJ, Day CL Jr. Long-term recurrence rates in previously untreated (primary) basal cell carcinoma: implications for patient follow-up. J Dermatol Surg Oncol 15:315-328, 1989.
3. Konig K, Riemann I. High-resolution multiphoton tomography of human skin with subcellular spatial resolution and picosecond time resolution. J Biomed Opt 8:432-439, 2003.

4. Lin SJ, Wu RJ, Tan HY, Lo W, Lin WC, Young TH, Hsu CJ, Chen JS, Jee SH, Dong CY. Evaluating cutaneous photoaging by use of multiphoton fluorescence and second harmonic generation microscopy. Opt Lett 30: 2275-2277, 2005.
5. Teng SW, Tan HY, Peng JL, Lin HH, Kim KH, Lo W, Sun Y, Lin WC, Lin SJ, Jee SH, So PTC, Dong CY. Multiphoton autofluorescence and second-harmonic generation (SHG) imaging of ex-vivo porcine eye. Invest Ophthalmol Vis Sci 47:1216-24, 2006.
6. Sun Y, Su J, Lo W, Lin SJ, Jee SH, Dong CY. Multiphoton polarization imaging of the stratum corneum and the dermis in ex-vivo human skin. Opt Express 11: 3377-3384, 2003.
7. W. Zipfel, R. Williams, R. Christie, A. Nikitin, B. Hyman, and W. Webb. Live tissue intrinsic emission microscopy using multiphoton-excited native fluorescence and second harmonic generation. P Natl Aca. Sci USA 100: 7075-7080, 2003.
8. Zoumi A, Yeh A, Tromberg BJ. Imaging cells and extracellular matrix in vivo by using second-harmonic generation and two-photon excited fluorescence. P Natl Aca. Sci USA 99, 11014-11019, 2002.
9. Brown E, McKee T, diTomaso E, Pluen A, Seed B, Boucher Y, Jain RK. Dynamic imaging of collagen and its modulation in tumors in vivo using second-harmonic generation. Nat Med 9: 796-800, 2003.
10. Campagnola PJ, Loew LM. Second-harmonic imaging microscopy for visualizing biomolecular arrays in cells, tissues and organisms. Nat Biotechnol 21:1356-1360, 2003.
11. Lin SJ, Hsiao CY, Sun Y, Lo W, WC Lin, Jan GJ, Jee SH, Dong CY. Monitoring the thermally induced structural transitions of collagen using second harmonic generation microscopy. Opt Lett 30:622-4, 2005.
12. Tan HY, Teng SW, Lo W, Lin WC, Lin SJ, Jee SH, Dong CY. Characterizing the thermally induced structural transitions to intact porcine eye I: Second harmonic generation imaging of cornea stroma. J Biomed Opt 10:54019, 2005.
13. Lin SJ, Lo W, Tan HY, Chan JY, Chen WL, Wang SH, Sun Y, Lin WC, Chen JS, Hsu CJ, Tjiu JW, Yu HS, Jee SH, Dong CY. Prediction of heat-induced collagen shrinkage by use of second harmonic generation microscopy. J Biomed Opt (accepted)
14. Nijssen A, Bakker Schut TC, Heule F, Caspers PJ, Hayes DP, Neumann MHA, Puppels GJ. Discriminating basal cell carcinoma from its surrounding tissue by

Raman spectroscopy. J Invest Dermatol 119:64-69, 2002.

15. Yucel T, Mutnal A, Fay K, Fligiel SE, Wang T, Johnson T, Baker SR, Varani J. Matrix metalloproteinase expression in basal cell carcinoma: relationship between enzyme profile and collagen fragmentation pattern. Exp Mol Pathol 79:151-60, 2005.